

Convergence investigation for the exponential matrix and mathematical layers in the static analysis of multilayered composite structures

Original

Convergence investigation for the exponential matrix and mathematical layers in the static analysis of multilayered composite structures / Brischetto, Salvatore; Torre, Roberto. - In: JOURNAL OF COMPOSITES SCIENCE. - ISSN 2504-477X. - 1:2(2017), pp. 1-15. [10.3390/jcs1020019]

Availability:

This version is available at: 11583/2697392 since: 2020-06-04T00:27:06Z

Publisher:

MDPI AG

Published

DOI:10.3390/jcs1020019

Terms of use:

This article is made available under terms and conditions as specified in the corresponding bibliographic description in the repository

Publisher copyright

(Article begins on next page)



Article

Convergence Investigation for the Exponential Matrix and Mathematical Layers in the Static Analysis of Multilayered Composite Structures

Salvatore Brischetto * and Roberto Torre

Department of Mechanical and Aerospace Engineering, Politecnico di Torino, Corso Duca degli Abruzzi, 24, 10129 Torino, Italy; roberto.torre@polito.it

* Correspondence: salvatore.brischetto@polito.it; Tel.: +39-011-090-6813; Fax: +39-011-090-6899

Received: 28 November 2017; Accepted: 13 December 2017; Published: 18 December 2017

Abstract: The exact three-dimensional analysis of a large group of geometries is accomplished here using the same formulation written in orthogonal mixed curvilinear coordinates. This solution is valid for plates, cylindrical shells, cylinders and spherical shells. It does not need specialized equations for each proposed geometry. It makes use of a formulation that is valid for spherical shells and automatically degenerates in the simpler geometries. Second order differential equations are reduced of an order redoubling the number of variables, and then they are solved via the exponential matrix method. Coefficients of equations vary through the thickness when shells are considered. M mathematical layers must be introduced into each physical layer to approximate the curvature. The correlation between M and the order of expansion N for the exponential matrix is analyzed in this paper in order to find their opportune combined values to obtain the exact results. As their effects may depend on different parameters, several geometries, lamination sequences, thickness ratios and imposed half-wave numbers are taken into consideration.

Keywords: plates; shells; static analysis; 3D elasticity solution; exact method; exponential matrix method; convergence study; mathematical layers

1. Introduction

Structural analysis in aerospace, mechanical and civil fields often considers complex geometries with any kind of boundary and load conditions, materials and, in the case of multilayered structures, lamination sequences. These problems have the possibility to be solved by means of even more refined numerical models, whose target is to draw more and more precisely the behavior of the structure taken into consideration, emphasizing its salient characteristics, thus allowing a parallel decrease of the weights involved and an increase in safety. A certain degree of confidence is acquired by a numerical model once it has been deeply validated by means of an opportune juxtaposition with an exact 3D model [1,2]. Plates and shells are the common geometries used by these exact models because of their particular simplicity and specific load and boundary conditions. They allow the closed solution of the differential equilibrium equations that govern the phenomenon. The closed solution is essential in this validation process as it is the only way to obtain a punctual description of displacement, strain and stress fields without any numerically-related deviations. Several 3D solutions for plates and shells have been proposed in the literature; however, all of them are characterized by a dedicated solution for the specific geometry involved. The present 3D solution poses the problem in orthogonal mixed curvilinear coordinates, thus allowing a unique formulation for the equations of motion for rectangular and square plates, cylindrical and spherical panels and closed cylinders. No simplifications are introduced; the equations are written and solved in the most general case, the spherical panel, and they automatically degenerate into the ones for simpler configurations. The differential equations are solved using the

exponential matrix method [3,4]. This approach needs constant coefficients. Several mathematical layers must be introduced in shell geometries to consider constant curvature-related terms.

Some of the most important 3D models proposed in the literature were developed for specific geometries. Pagano deeply analyzed the problem of the mechanical response of composite laminated structures. The cylindrical bending of composite laminated plates was studied in [5] while an exact solution for rectangular and square, composite and sandwich plates was proposed in [6], where the maximum stresses and deflections were investigated. More general load cases in cylindrical bending were considered in [7]. Demasi [8] found the exact three-dimensional solution for isotropic rectangular plates using the mixed form of Hooke's law, and he showed the closed form expression for stresses and displacements of a rectangular plate under sinusoidal load. Fan and Ye [9] analyzed the statics and the dynamics of plates with orthotropic layers overcoming the problem of increasing the number of equations to be solved with the number of the layers. Actually, the free vibration analysis of multilayered plates was proposed by several authors. Srinivas et al. [10] proposed a three-dimensional solution for the free vibration of simply-supported, homogeneous and thick laminated rectangular plates made of isotropic materials. Circular and annular plates were studied by Taher et al. [11]; the first frequencies were found for different thickness ratios and boundary conditions. Hosseini-Hashemi et al. [12] used two different displacement fields to study the in-plane and the out-of-plane vibrations of a rectangular homogeneous plate, coated by a functionally graded layer. Messina [13] used the exponential matrix method to solve the three-dimensional equations of equilibrium, written in a Cartesian coordinate system, for cross-ply laminated rectangular plates. The free vibration frequencies, stresses and deflections were presented. On the other side, Ye [14] preferred to start from the recursive solution proposed in [9] to study the free vibration of cross-ply plates. Other authors proposed different formulations valid for shells with an unavoidable increase in complexity with respect to the ones developed for flat cases. Varadan and Bhaskar [15] studied the effects of harmonic loads applied to cross-ply cylinders; Fan and Zhang [16] looked for an exact solution of the equations of elasticity in a curvilinear coordinate system. Also in these cases, several solutions have been proposed for the free vibration analysis. The free frequencies of simply supported composite mono and doubly-curved shells were found by Huang [17] using the power series method. A further example for the use of the exponential matrix method to solve the 3D equilibrium equations may be found in [18], where Soldatos and Ye wrote the equations in cylindrical coordinates, in order to calculate the free frequencies of angle-ply multilayered cylinders. Khalili et al. [19] solved the free vibration problem for isotropic cylinders with different boundary conditions by means of the Galerkin method and writing the equations using the Hamilton's principle.

Although several solutions were already proposed, all of them were written for a specific kind of geometry, with a lack of universality. In the present 3D solution, the equilibrium equations are written in orthogonal mixed curvilinear coordinates. The first author's past works extensively described all the details of the proposed 3D formulation used for the free vibration analysis of one-layered and multilayered spherical, cylindrical and flat one-layered panels [20,21]. The same idea was extended to the static problem of shells subjected to harmonic loads on the top and bottom surfaces in [22]. More general load combinations were considered in [23]. In conclusion, this formulation can be used for the static and dynamic analysis of plates, cylinders and cylindrical/spherical shell panels. The method involves some parametric coefficients that depend on the radii of curvature and on the thickness coordinate z . These coefficients allow the equations to degenerate into the ones for simpler geometries when one or both the radii of curvature are infinite. The exact/closed solution is obtained assuming a harmonic form for displacement components and loads, and considering the structure as simply supported. A simple stratagem of redoubling the number of variables allows the reduction to a system of first order partial differential equations. The exponential matrix method is then used to solve the reduced equation system across the thickness coordinate z . In order to reach the solution, an opportune expansion order N must be chosen for the exponential matrix. This method has constant coefficients for the first order partial differential equations in the plate case. When at least one radius

of curvature is different from infinite, the parametric coefficients become functions of the thickness coordinate z , and the coefficients for equations in each physical layer vary in z . In these cases, several mathematical layers M must be introduced to approximate the curvature terms and to solve the system. A convergence analysis for the introduced number M of mathematical layers and for the order N used in the expansion of the exponential matrix in the case of plates and shells (with different dimensions, thickness ratios, lamination sequences and geometries) is proposed in this paper. A similar study was already proposed for the free vibration analysis of sandwich and multilayered plates, cylinders and cylindrical/spherical shell panels in [24] and for functionally graded plates and shells in [25]. The opportune combination of M and N values is essential in order to guarantee the convergence and to optimize the model in terms of convergence speed. As shown in [25,26], the use of mathematical layers is also useful when functionally graded materials are taken into consideration because it allows for better considering the evolution of the mechanical properties through the thickness.

2. Three-Dimensional Equilibrium Equations for Static Analysis

Notations, reference systems and geometrical parameters for shell structures in the most general case are indicated in Figures 1 and 2. Ω_0 is the middle surface of the shell, defined as the locus of points that fall midway between the bottom and the top surfaces. The reference system (α, β, z) is mixed curvilinear and orthogonal. Its origin is located in a corner. z is normal to the middle surface, heading towards the upper surface. α and β lie on it. h is the thickness of the shell, z varies from $-h/2$ to $h/2$. For shells with constant radii of curvature in both directions, the following parametric quantities can be defined:

$$H_\alpha = \left(1 + \frac{z}{R_\alpha}\right) = \left(1 + \frac{\tilde{z} - h/2}{R_\alpha}\right), \quad H_\beta = \left(1 + \frac{z}{R_\beta}\right) = \left(1 + \frac{\tilde{z} - h/2}{R_\beta}\right), \quad H_z = 1. \quad (1)$$

In Equation (1), R_α and R_β are the radii of curvature referred to the mid-surface evaluated in α and β directions, respectively. H_α and H_β continuously vary across the thickness following the thickness coordinate z or \tilde{z} .

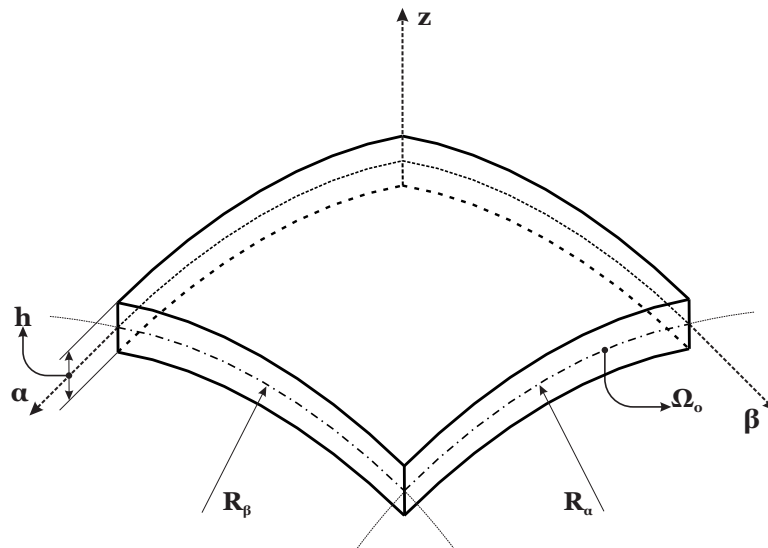


Figure 1. Notations, reference system and geometrical parameters for shell structures.

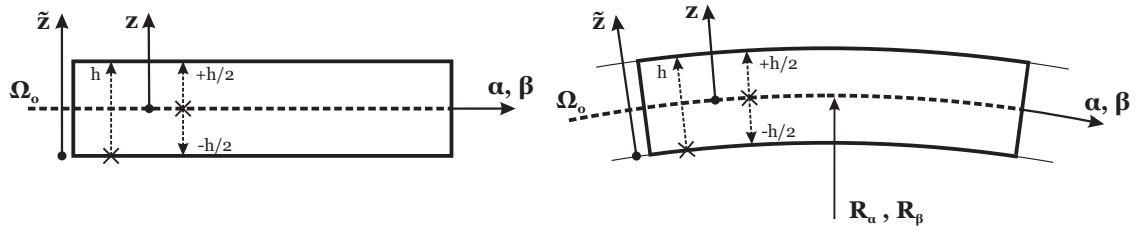


Figure 2. Thickness coordinates z and \tilde{z} , and reference systems for shell structures.

Using the above coefficients, the static analysis of a spherical shell with a constant radii of curvature in α and β directions, made of a generic number N_L of layers, can be done writing for each k layer the following differential equations of equilibrium:

$$H_\beta \frac{\partial \sigma_{\alpha\alpha}^k}{\partial \alpha} + H_\alpha \frac{\partial \sigma_{\alpha\beta}^k}{\partial \beta} + H_\alpha H_\beta \frac{\partial \sigma_{\alpha z}^k}{\partial z} + \left(\frac{2H_\beta}{R_\alpha} + \frac{H_\alpha}{R_\beta} \right) \sigma_{\alpha z}^k = 0, \tag{2}$$

$$H_\beta \frac{\partial \sigma_{\alpha\beta}^k}{\partial \alpha} + H_\alpha \frac{\partial \sigma_{\beta\beta}^k}{\partial \beta} + H_\alpha H_\beta \frac{\partial \sigma_{\beta z}^k}{\partial z} + \left(\frac{2H_\alpha}{R_\beta} + \frac{H_\beta}{R_\alpha} \right) \sigma_{\beta z}^k = 0, \tag{3}$$

$$H_\beta \frac{\partial \sigma_{\alpha z}^k}{\partial \alpha} + H_\alpha \frac{\partial \sigma_{\beta z}^k}{\partial \beta} + H_\alpha H_\beta \frac{\partial \sigma_{zz}^k}{\partial z} - \frac{H_\beta}{R_\alpha} \sigma_{\alpha\alpha}^k - \frac{H_\alpha}{R_\beta} \sigma_{\beta\beta}^k + \left(\frac{H_\beta}{R_\alpha} + \frac{H_\alpha}{R_\beta} \right) \sigma_{zz}^k = 0. \tag{4}$$

k indicates the physical layer, so it may vary between 1 (at the bottom) and N_L (at the top); symbol ∂ stands for the partial derivatives. $(\sigma_{\alpha\alpha}^k, \sigma_{\beta\beta}^k, \sigma_{zz}^k, \sigma_{\beta z}^k, \sigma_{\alpha z}^k, \sigma_{\alpha\beta}^k)$ are the six stress components. R_α, R_β and H_α, H_β have been described before. A less specialized form of Equations (2)–(4), valid for shells with variable radii of curvature, may be found in [2,27]. In order to write Equations (2)–(4) in displacement form, the geometrical relationships and the constitutive equations must be introduced. A simplified expression of the geometrical relationships in orthogonal mixed curvilinear coordinates (see [27,28]) is possible when they are written for shells with constant radii of curvature. $(\epsilon_{\alpha\alpha}^k, \epsilon_{\beta\beta}^k, \epsilon_{zz}^k, \gamma_{\beta z}^k, \gamma_{\alpha z}^k, \gamma_{\alpha\beta}^k)$ are the six strain components when the three displacement components u, v , and w in direction α, β, z , respectively, have been introduced:

$$\epsilon_{\alpha\alpha}^k = \frac{1}{H_\alpha} \frac{\partial u^k}{\partial \alpha} + \frac{w^k}{H_\alpha R_\alpha}, \tag{5}$$

$$\epsilon_{\beta\beta}^k = \frac{1}{H_\beta} \frac{\partial v^k}{\partial \beta} + \frac{w^k}{H_\beta R_\beta}, \tag{6}$$

$$\epsilon_{zz}^k = \frac{\partial w^k}{\partial z}, \tag{7}$$

$$\gamma_{\beta z}^k = \frac{1}{H_\beta} \frac{\partial w^k}{\partial \beta} + \frac{\partial v^k}{\partial z} - \frac{v^k}{H_\beta R_\beta}, \tag{8}$$

$$\gamma_{\alpha z}^k = \frac{1}{H_\alpha} \frac{\partial w^k}{\partial \alpha} + \frac{\partial u^k}{\partial z} - \frac{u^k}{H_\alpha R_\alpha}, \tag{9}$$

$$\gamma_{\alpha\beta}^k = \frac{1}{H_\alpha} \frac{\partial v^k}{\partial \alpha} + \frac{1}{H_\beta} \frac{\partial u^k}{\partial \beta}. \tag{10}$$

The field covered by Equations (5)–(10) is wide. They are written for a generic spherical shell with constant radii of curvature. When one of the two radii of curvature R_α or R_β is infinite (H_α or H_β equal to 1), they automatically degenerate into equations for cylinders and cylindrical shells. When $R_\alpha = R_\beta = \infty$ (so $H_\alpha = H_\beta = 1$), they work for the plate case. The connection between the six stress components and the six strain components is obtained by means of the linear elastic

constitutive equations. A closed form solution of Equations (2)–(4) is possible only considering orthotropic materials, with fibre orientation angle θ equal to 0° or 90° in the structure reference system. These conditions lead to a simplified link between stress and strain vectors:

$$\begin{bmatrix} \sigma_{\alpha\alpha}^k \\ \sigma_{\beta\beta}^k \\ \sigma_{zz}^k \\ \sigma_{\beta z}^k \\ \sigma_{\alpha z}^k \\ \sigma_{\alpha\beta}^k \end{bmatrix} = \begin{bmatrix} C_{11}^k & C_{12}^k & C_{13}^k & 0 & 0 & 0 \\ C_{12}^k & C_{22}^k & C_{23}^k & 0 & 0 & 0 \\ C_{13}^k & C_{23}^k & C_{33}^k & 0 & 0 & 0 \\ 0 & 0 & 0 & C_{44}^k & 0 & 0 \\ 0 & 0 & 0 & 0 & C_{55}^k & 0 \\ 0 & 0 & 0 & 0 & 0 & C_{66}^k \end{bmatrix} \begin{bmatrix} \epsilon_{\alpha\alpha}^k \\ \epsilon_{\beta\beta}^k \\ \epsilon_{zz}^k \\ \gamma_{\beta z}^k \\ \gamma_{\alpha z}^k \\ \gamma_{\alpha\beta}^k \end{bmatrix} \quad (11)$$

Details about the full version of the matrix of elastic coefficients may be found in [29,30].

For the closed solution of the Equations (2)–(4), a harmonic form for the three displacement components is assumed:

$$u^k(\alpha, \beta, z) = U^k(z)\cos(\bar{\alpha}\alpha)\sin(\bar{\beta}\beta), \quad (12)$$

$$v^k(\alpha, \beta, z) = V^k(z)\sin(\bar{\alpha}\alpha)\cos(\bar{\beta}\beta), \quad (13)$$

$$w^k(\alpha, \beta, z) = W^k(z)\sin(\bar{\alpha}\alpha)\sin(\bar{\beta}\beta). \quad (14)$$

U^k , V^k and W^k , are the displacement amplitudes in α , β and z directions, respectively. a and b are the shell dimensions, evaluated in the mid-surface Ω_0 , in α and β directions, respectively. p and q are the half-wave numbers in the same directions. The coefficients of the two trigonometric functions are defined as $\bar{\alpha} = \frac{p\pi}{a}$ and $\bar{\beta} = \frac{q\pi}{b}$. Combining the constitutive Equation (11) with the geometrical relations (5)–(10) and the harmonic form of the three displacements (12)–(14) into Equations (2)–(4), a displacement form of the equilibrium equations may be obtained in terms of the amplitudes of the displacements and their appropriate derivatives. Expressing in a compact form the partial derivatives $\frac{\partial}{\partial\alpha}$, $\frac{\partial}{\partial\beta}$ and $\frac{\partial}{\partial z}$ with the subscripts α , β and z , the differential equations of equilibrium in displacement form for a generic n layer are:

$$\begin{aligned} & \left(-\frac{C_{55}^n H_\beta}{H_\alpha R_\alpha^2} - \frac{C_{55}^n}{R_\alpha R_\beta} - \bar{\alpha}^2 \frac{C_{11}^n H_\beta}{H_\alpha} - \bar{\beta}^2 \frac{C_{66}^n H_\alpha}{H_\beta}\right)U^n + (-\bar{\alpha}\bar{\beta}C_{12}^n - \bar{\alpha}\bar{\beta}C_{66}^n)V^n + \left(\bar{\alpha} \frac{C_{11}^n H_\beta}{H_\alpha R_\alpha} + \bar{\alpha} \frac{C_{12}^n}{R_\beta} + \right. \\ & \left. \bar{\alpha} \frac{C_{55}^n H_\beta}{H_\alpha R_\alpha} + \bar{\alpha} \frac{C_{55}^n}{R_\beta}\right)W^n + \left(\frac{C_{55}^n H_\beta}{R_\alpha} + \frac{C_{55}^n H_\alpha}{R_\beta}\right)U_{,z}^n + (\bar{\alpha}C_{13}^n H_\beta + \bar{\alpha}C_{55}^n H_\beta)W_{,z}^n + (C_{55}^n H_\alpha H_\beta)U_{,zz}^n = 0, \quad (15) \end{aligned}$$

$$\begin{aligned} & (-\bar{\alpha}\bar{\beta}C_{66}^n - \bar{\alpha}\bar{\beta}C_{12}^n)U^n + \left(-\frac{C_{44}^n H_\alpha}{H_\beta R_\beta^2} - \frac{C_{44}^n}{R_\alpha R_\beta} - \bar{\alpha}^2 \frac{C_{66}^n H_\beta}{H_\alpha} - \bar{\beta}^2 \frac{C_{22}^n H_\alpha}{H_\beta}\right)V^n + \left(\bar{\beta} \frac{C_{44}^n H_\alpha}{H_\beta R_\beta} + \bar{\beta} \frac{C_{44}^n}{R_\alpha} + \right. \\ & \left. \bar{\beta} \frac{C_{22}^n H_\alpha}{H_\beta R_\beta} + \bar{\beta} \frac{C_{12}^n}{R_\alpha}\right)W^n + \left(\frac{C_{44}^n H_\alpha}{R_\beta} + \frac{C_{44}^n H_\beta}{R_\alpha}\right)V_{,z}^n + (\bar{\beta}C_{44}^n H_\alpha + \bar{\beta}C_{23}^n H_\alpha)W_{,z}^n + (C_{44}^n H_\alpha H_\beta)V_{,zz}^n = 0, \quad (16) \end{aligned}$$

$$\begin{aligned} & \left(\bar{\alpha} \frac{C_{55}^n H_\beta}{H_\alpha R_\alpha} - \bar{\alpha} \frac{C_{13}^n}{R_\beta} + \bar{\alpha} \frac{C_{11}^n H_\beta}{H_\alpha R_\alpha} + \bar{\alpha} \frac{C_{12}^n}{R_\beta}\right)U^n + \left(\bar{\beta} \frac{C_{44}^n H_\alpha}{H_\beta R_\beta} - \bar{\beta} \frac{C_{23}^n}{R_\alpha} + \bar{\beta} \frac{C_{22}^n H_\alpha}{H_\beta R_\beta} + \bar{\beta} \frac{C_{12}^n}{R_\alpha}\right)V^n + \left(\frac{C_{13}^n}{R_\alpha R_\beta} + \right. \\ & \left. \frac{C_{23}^n}{R_\alpha R_\beta} - \frac{C_{11}^n H_\beta}{H_\alpha R_\alpha^2} - \frac{2C_{12}^n}{R_\alpha R_\beta} - \frac{C_{22}^n H_\alpha}{H_\beta R_\beta^2} - \bar{\alpha}^2 \frac{C_{55}^n H_\beta}{H_\alpha} - \bar{\beta}^2 \frac{C_{44}^n H_\alpha}{H_\beta}\right)W^n + (-\bar{\alpha}C_{55}^n H_\beta - \bar{\alpha}C_{13}^n H_\beta)U_{,z}^n + \quad (17) \end{aligned}$$

$$(-\bar{\beta}C_{44}^n H_\alpha - \bar{\beta}C_{23}^n H_\alpha)V_{,z}^n + \left(\frac{C_{33}^n H_\beta}{R_\alpha} + \frac{C_{33}^n H_\alpha}{R_\beta}\right)W_{,z}^n + (C_{33}^n H_\alpha H_\beta)W_{,zz}^n = 0.$$

As already seen for the geometrical relationships, the field covered by Equations (15)–(17) is wide because they are written for a generic spherical shell, but when one radius of curvature R_α or R_β is infinite (H_α or H_β equal to 1), they automatically degenerate into equations for cylinders and cylindrical shells. Likewise, when $R_\alpha = R_\beta = \infty$ ($H_\alpha = H_\beta = 1$), they work for the plate case.

The whole formulation that leads to Equations (15)–(17) takes into consideration the shell geometry via the parametric coefficients H_α and H_β , which depend on the thickness coordinate z . As a result, the coefficients that multiply displacements and their derivatives in z are not constant. Just in the plate case, as both the radii of curvature R_α and R_β are infinite and $H_\alpha = H_\beta = 1$, the coefficients of Equations (15)–(17) become constant and the exponential matrix method may be used directly to solve the system. In order to calculate H_α and H_β , each physical layer k is divided in a certain number M of mathematical layers j . This makes the structure being constituted by $T = N_L \times M$ layers, where total index may be expressed by $n = k \times j$. The coefficients are thus constant as they are evaluated with R_α and R_β measured on the mid-surface of the whole shell Ω_0 , and H_α and H_β are calculated in the middle of each n layer. An example of the introduction of mathematical layers into the shell geometry is presented in Figure 3, a three layered shell (three physical layers) is shown considering a number $M = 1$ and $M = 5$ of mathematical layers for each physical layer.

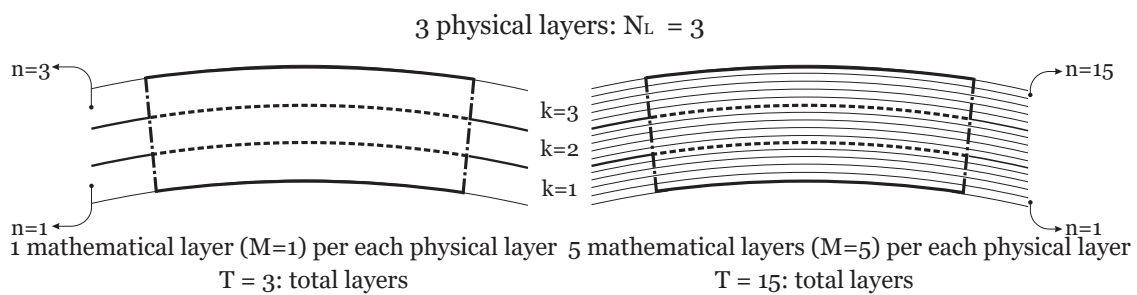


Figure 3. Three-layered structures, examples for the use of M mathematical layers.

3. Use of the Exponential Matrix and Mathematical Layers in the Solution of 3D Equilibrium Equations

Assigning to each block in parentheses of Equations (15)–(17) a coefficient A_s^n (with s varying from 1 to 19), the system may be compacted as:

$$A_1^n U^n + A_2^n V^n + A_3^n W^n + A_4^n U_{,z}^n + A_5^n W_{,z}^n + A_6^n U_{,zz}^n = 0, \tag{18}$$

$$A_7^n U^n + A_8^n V^n + A_9^n W^n + A_{10}^n V_{,z}^n + A_{11}^n W_{,z}^n + A_{12}^n V_{,zz}^n = 0, \tag{19}$$

$$A_{13}^n U^n + A_{14}^n V^n + A_{15}^n W^n + A_{16}^n U_{,z}^n + A_{17}^n V_{,z}^n + A_{18}^n W_{,z}^n + A_{19}^n W_{,zz}^n = 0. \tag{20}$$

These equations constitute a system of second order differential equations. A simple method of reducing its order to the first one is described in [3,31] and it may be summarized as a redoubling of the involved variables. In the first author’s past works [20,21], a detailed description of this approach can be found. The compact form of the reduced system of first order partial differential equations is:

$$D^n \frac{\partial \mathbf{U}^n}{\partial \bar{z}} = A^n \mathbf{U}^n, \tag{21}$$

where $\frac{\partial \mathbf{U}^n}{\partial \bar{z}} = \mathbf{U}^{n'}$ and $\mathbf{U}^n = [U^n \ V^n \ W^n \ U^{n'} \ V^{n'} \ W^{n'}]$. A further development of Equation (21) is:

$$\mathbf{U}^{n'} = A^{n*} \mathbf{U}^n, \tag{22}$$

where $A^{n*} = D^{n-1} A^n$.

Equation (22) is a system of first order differential equations that can be easily solved as shown in [31,32] with the exponential matrix method:

$$\mathbf{U}^n(\bar{z}^n) = \exp(A^{n*} \bar{z}^n) \mathbf{U}^n(0) \quad \text{with } \bar{z}^n \in [0, h^n]. \tag{23}$$

\bar{z}^n is the thickness coordinate of each mathematical layer and it varies from 0 at its bottom to h^n at its top (see Figure 2). The exponential matrix for each n layer, with constant coefficients A_s^n , is calculated with $\bar{z}^n = h^n$:

$$A^{n**} = \exp(A^{n*}h^n) = I + A^{n*}h^n + \frac{A^{n*2}}{2!}h^{n2} + \frac{A^{n*3}}{3!}h^{n3} + \dots + \frac{A^{n*N}}{N!}h^{nN}. \quad (24)$$

I is the 6×6 identity matrix. The fast convergence ratio for increasing values of N and its low computational time consumption were shown in [4].

The relation in Equation (23), evaluated at $\bar{z}^n = h^n$, allows for linking the displacements (and their derivatives) within the bottom and the top of the same layer n . The interlaminar continuity of displacements and transverse shear and normal stresses may be imposed at each interface. These quantities evaluated at the bottom of the n layer must be the same as those evaluated at the top of the $(n - 1)$ layer:

$$u_b^n = u_t^{n-1}, \quad v_b^n = v_t^{n-1}, \quad w_b^n = w_t^{n-1}, \quad (25)$$

$$\sigma_{zzb}^n = \sigma_{zzt}^{n-1}, \quad \sigma_{\alpha zb}^n = \sigma_{\alpha zt}^{n-1}, \quad \sigma_{\beta zb}^n = \sigma_{\beta zt}^{n-1}. \quad (26)$$

Conditions in Equations (25)–(26) may be expressed via $N_L \times M - 1$ transfer matrices $T^{n-1,n}$ calculated for each interface. Details about their determination can be found in the first author’s past works [20–26].

Plates and shells taken into consideration are supposed to have simply supported edges; moreover they can be loaded at the top (subscript t) and/or at the bottom (subscript b) of the whole laminated structure:

$$w = v = 0, \quad \sigma_{\alpha\alpha} = 0 \quad \text{for} \quad \alpha = 0, a, \quad (27)$$

$$w = u = 0, \quad \sigma_{\beta\beta} = 0 \quad \text{for} \quad \beta = 0, b, \quad (28)$$

$$\sigma_{zz} = p_{zb}, \quad \sigma_{\alpha z} = p_{\alpha b}, \quad \sigma_{\beta z} = p_{\beta b} \quad \text{for} \quad z = -h/2 \quad \text{or} \quad \bar{z} = 0, \quad (29)$$

$$\sigma_{zz} = p_{zt}, \quad \sigma_{\alpha z} = p_{\alpha t}, \quad \sigma_{\beta z} = p_{\beta t} \quad \text{for} \quad z = +h/2 \quad \text{or} \quad \bar{z} = h. \quad (30)$$

Grouping the loads applied on the bottom and the ones applied on the top in two separate vectors and specifying the stresses in terms of displacements and their derivatives, Equations (29) and (30), may be written as:

$$B^T(h^T)U^T(h^T) = P_t^T, \quad (31)$$

$$B^1(0)U^1(0) = P_b^1, \quad (32)$$

where

$$P_t^T = \begin{bmatrix} P_{zt}^T \\ P_{\beta t}^T \\ P_{\alpha t}^T \end{bmatrix}, \quad P_b^1 = \begin{bmatrix} P_{zb}^1 \\ P_{\beta b}^1 \\ P_{\alpha b}^1 \end{bmatrix}, \quad (33)$$

and $U^1(0)$, $U^T(h^T)$ are U vector calculated at the bottom of the whole multilayered structure (which means layer 1 and coordinate $\bar{z}^1 = 0$), and at the top of the entire structure (which means layer T and $\bar{z}^T = h_T$).

Introducing recursively Equations (25) and (26) into Equation (23), Equations (31) and (32) may be grouped into a general algebraic system:

$$EU^1(0) = P, \quad (34)$$

with $\mathbf{P} = [P_{zt}^T \ P_{\beta t}^T \ P_{\alpha t}^T \ P_{zb}^1 \ P_{\beta b}^1 \ P_{\alpha b}^1]^T$.

Equation (34) allows for finding the vector $\mathbf{U}^1(0)$, containing the values of the three displacement components and their respective derivatives at the bottom. The values assumed by vector \mathbf{U} can be calculated at each value of the thickness coordinate z by means of Equations (23), (25) and (26). All of the details and the missing steps to reach the final solution may be found in the first author’s past works [22,33].

4. Results

The results presented in this section are given in order to find the best combination between the order of expansion N of the exponential matrix A^{n**} and the number M of mathematical layers used to solve the differential equations written for shell geometries with assumed constant coefficients. Depending on the case, the structure may have a certain number of physical layers; each physical layer can be divided into M mathematical layers, having the same thickness. An example on how a three-layered structure may be divided into a certain number of mathematical layers is presented in Figure 3.

Results are presented in terms of no-dimensional displacements and/or stresses, with a specific factor for each case. When the present 3D solution converges, the results are indicated in bold. The cases presented hereinafter consider simply supported rectangular plates, cylindrical shell panels, cylinders and spherical shell panels. A summary of the loads, geometrical data and materials for the analyzed cases can be found in Tables 1 and 2. All these geometries have been considered as multi-layered embedding a fibre reinforced composite material, whose properties are indicated in Table 1. Different lamination sequences were considered, a symmetric cross ply laminate is taken into account in Cases 1, 3 and 4; an antisymmetric case is investigated in Case 2.

Table 1. Material data for the employed composite layers.

Composite for Cases 1–4	
E_1 [psi]	25×10^6
E_2 [psi]	1×10^6
E_3 [psi]	1×10^6
G_{12} [psi]	0.5×10^6
G_{13} [psi]	0.5×10^6
G_{23} [psi]	0.2×10^6
ν_{12}	0.25
ν_{13}	0.25
ν_{23}	0.25

Table 2. Load and geometrical data for the analyzed cases. Case 1 takes into consideration the rectangular composite plate proposed by Pagano [6], Case 2 is about the composite laminated cylindrical panel proposed by Ren [34], Case 3 regards the composite laminated cylinder by Varadan and Bhaskar [15], and Case 4 deals with the composite laminated spherical panel proposed by Fan and Zhang [35].

Parameter	Case 1 [6]	Case 2 [34]	Case 3 [15]	Case 4 [35]
a [in]	1	$\frac{\pi}{3}R_\alpha$	$2\pi R_\alpha$	10
b [in]	3	1	40	10
R_α [in]	∞	10	10	10
R_β [in]	∞	∞	∞	10
h_1	$h/3$	$h/2$	$h/3$	$h/3$
h_2	$h/3$	$h/2$	$h/3$	$h/3$
h_3	$h/3$	-	$h/3$	$h/3$
lamination	$0^\circ/90^\circ/0^\circ$	$90^\circ/0^\circ$	$0^\circ/90^\circ/0^\circ$	$0^\circ/90^\circ/0^\circ$
P_z [psi]	1 (top)	1 (top)	1 (bottom)	1 (top)
p [-]	1	1	8	1
q [-]	1	0	1	1

Case 1 was proposed by Pagano in [6] for the exact 3D solution of a simply supported rectangular composite laminated plate. The material properties are indicated in Table 1. The load, the geometry and the lamination scheme are indicated in the first column of Table 2. Results are expressed in terms of no-dimensional displacements and stresses:

$$(\bar{w}) = \frac{100E_2^{comp}w}{P_z h(a/h)^4}, \tag{35}$$

$$(\bar{\sigma}_{\alpha z}) = \frac{\sigma_{\alpha z}}{P_z(a/h)}. \tag{36}$$

Case 2 was proposed by Ren in [34] for the exact 3D solution of a simply supported composite laminated cylindrical panel. The dimensions, thickness values, load conditions and lamination scheme are proposed in the second column of Table 2. Each layer has the elastic properties as proposed in Table 1. Results are shown in terms of no-dimensional displacements and stresses:

$$(\bar{w}) = \frac{10E_2^{comp}w}{P_z h(R_\alpha/h)^4}, \tag{37}$$

$$(\bar{\sigma}_{\alpha\alpha}) = \frac{\sigma_{\alpha\alpha}}{P_z(R_\alpha/h)^2}. \tag{38}$$

Case 3 was investigated by Varadan and Bhaskar in [15] for the exact 3D solution of a simply supported composite laminated cylinder. The in-plane dimensions, the considered thickness values, the mechanical load and the given values of half-wave numbers (p, q) are shown in the third column of Table 2. Table 1 shows the material properties. Results are calculated in terms of no-dimensional displacements and stresses:

$$(\bar{w}) = -\frac{10E_1^{comp}w}{P_z h(R_\alpha/h)^4}, \tag{39}$$

$$(\bar{\sigma}_{zz}) = -\sigma_{zz}. \tag{40}$$

The last considered geometry for the Case 4 was proposed by Fan and Zhang in [35] for the exact 3D solution of a simply supported composite laminated spherical shell. The radii of curvature, the in-plane dimensions, the considered thickness values, the mechanical load and the half-wave numbers (p, q) are proposed in the fourth column of Table 2 (see Table 1 for elastic material properties). Results are expressed in terms of no-dimensional displacements:

$$(\bar{w}) = \frac{10^3 E_2^{comp} h^3 w}{P_z a^4}. \tag{41}$$

Table 3 shows the displacement \bar{w} and the stress $\bar{\sigma}_{\alpha z}$ for the three-layered rectangular plate. Both of the quantities are given as dimensionless values and calculated in the middle. The displacement is evaluated for a plate whose thickness ratio is $a/h = 4$, while the stress is for a structure with $a/h = 10$. In this case, the introduction of M mathematical layer is unnecessary. Actually, when $M = 1$, the convergence is reached just by means of an opportune increase of the order of expansion N . For the thinner plate, $N = 5$ is sufficient for the stress to reach the convergence; the thicker plate needs an higher value ($N = 8$). The introduction of a certain number M of mathematical layers helps to reduce the expansion order N . However, for the computational point of view, the first procedure is more convenient. The comparison underlines the fact that an increase in N value is needed as the thickness increases with respect to the shell dimensions. The convergence of the stress $\bar{\sigma}_{\alpha z}$ with increasing values of M is shown in Figure 4 for several orders of expansion N .

Table 3. Case 1. Rectangular laminated composite plate. Displacement \bar{w} for thickness ratio $a/h = 4$ and stress $\bar{\sigma}_{\alpha z}$ for thickness ratio $a/h = 10$, both evaluated in the middle and given as dimensionless values. Each physical layer ($N_L=3$) is divided into M mathematical layers. 3D reference solution by Pagano [6].

$\bar{w}(a/2, b/2, 0); a/h = 4$												
	$N = 1$	$N = 2$	$N = 3$	$N = 4$	$N = 5$	$N = 6$	$N = 7$	$N = 8$	$N = 9$	$N = 10$	$N = 11$	$N = 12$
$M = 1$	3.07	1.82	3.31	2.60	2.89	2.80	2.83	2.82	2.82	2.82	2.82	2.82
$M = 2$	2.82	2.64	2.84	2.81	2.82	2.82	2.82	2.82	2.82	2.82	2.82	2.82
$M = 5$	2.83	2.80	2.82	2.82	2.82	2.82	2.82	2.82	2.82	2.82	2.82	2.82
$M = 10$	2.83	2.82	2.82	2.82	2.82	2.82	2.82	2.82	2.82	2.82	2.82	2.82
$M = 20$	2.82	2.82	2.82	2.82	2.82	2.82	2.82	2.82	2.82	2.82	2.82	2.82
$M = 40$	2.82	2.82	2.82	2.82	2.82	2.82	2.82	2.82	2.82	2.82	2.82	2.82
$M = 60$	2.82	2.82	2.82	2.82	2.82	2.82	2.82	2.82	2.82	2.82	2.82	2.82
$M = 80$	2.82	2.82	2.82	2.82	2.82	2.82	2.82	2.82	2.82	2.82	2.82	2.82
$M = 100$	2.82	2.82	2.82	2.82	2.82	2.82	2.82	2.82	2.82	2.82	2.82	2.82

$\bar{\sigma}_{\alpha z}(0, b/2, 0); a/h = 10$												
	$N = 1$	$N = 2$	$N = 3$	$N = 4$	$N = 5$	$N = 6$	$N = 7$	$N = 8$	$N = 9$	$N = 10$	$N = 11$	$N = 12$
$M = 1$	0.474	0.324	0.431	0.417	0.420	0.420	0.420	0.420	0.420	0.420	0.420	0.420
$M = 2$	0.432	0.396	0.421	0.420	0.420	0.420	0.420	0.420	0.420	0.420	0.420	0.420
$M = 5$	0.422	0.416	0.420	0.420	0.420	0.420	0.420	0.420	0.420	0.420	0.420	0.420
$M = 10$	0.421	0.419	0.420	0.420	0.420	0.420	0.420	0.420	0.420	0.420	0.420	0.420
$M = 20$	0.420	0.420	0.420	0.420	0.420	0.420	0.420	0.420	0.420	0.420	0.420	0.420
$M = 40$	0.420	0.420	0.420	0.420	0.420	0.420	0.420	0.420	0.420	0.420	0.420	0.420
$M = 60$	0.420	0.420	0.420	0.420	0.420	0.420	0.420	0.420	0.420	0.420	0.420	0.420
$M = 80$	0.420	0.420	0.420	0.420	0.420	0.420	0.420	0.420	0.420	0.420	0.420	0.420
$M = 100$	0.420	0.420	0.420	0.420	0.420	0.420	0.420	0.420	0.420	0.420	0.420	0.420

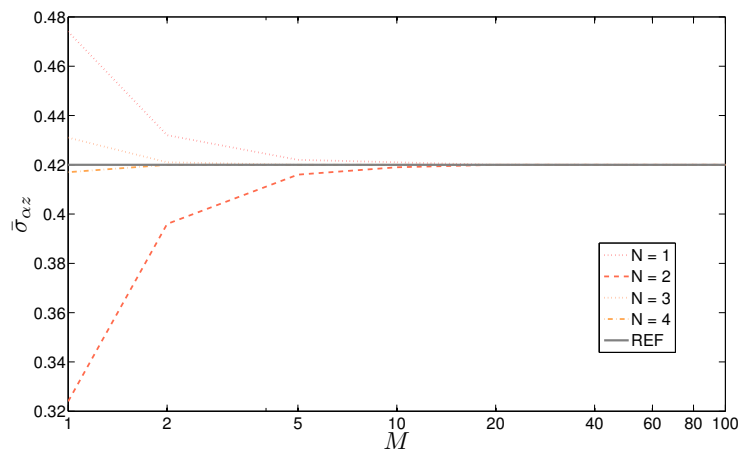


Figure 4. Case 1, simply supported rectangular laminated composite plate with thickness ratio $a/h = 10$. Stress $\bar{\sigma}_{\alpha z}$ vs. number M of mathematical layers introduced for different orders of expansion N for the exponential matrix. REF means a 3D solution by Pagano [6].

The displacement \bar{w} and the stress $\bar{\sigma}_{\alpha\alpha}$ for the two layered cylindrical shell are shown in Table 4. The displacement is considered in the middle, and the stress is on the top surface of the shell. A thick ($R_\alpha/h = 4$) and a moderately thick ($R_\alpha/h = 10$) panel are considered. All the values are given as dimensionless. This case remarks on the need for the introduction of mathematical layers when the curvature is introduced. In both cases, an increase in the order of expansion N of the exponential matrix until 12 is totally ineffective until $M = 10$ mathematical layers are introduced into each physical layer. Under these circumstances, $N = 3$ is then sufficient to get the exact result for both moderately thick and thick shells. Convergence speed seems to be the same for different thickness ratios, while a slower convergence would have been expected for the thicker shell. This effect is tempered by the fact that the comparison is made on two heterogeneous quantities. As the displacements are a direct

output of this formulation, they would generally converge faster than the stresses, which come from a combination of displacements and their derivatives. The results presented in Table 4 are shown in Figure 5 for the stress $\bar{\sigma}_{\alpha\alpha}$ with a progressive increase of the order of expansion for the exponential matrix until $N = 6$.

Table 4. Case 2. Composite laminated cylindrical shell. Displacement \bar{w} for thickness ratio $R_\alpha/h = 4$ evaluated in the middle and stress $\bar{\sigma}_{\alpha\alpha}$ for thickness ratio $R_\alpha/h = 10$ evaluated at the top, both given as dimensionless values. Each physical layer ($N_L = 2$) is divided into M mathematical layers. 3D reference solution by Ren [34].

$\bar{w}(a/2, b/2, 0); R_\alpha/h = 4$												
	$N = 1$	$N = 2$	$N = 3$	$N = 4$	$N = 5$	$N = 6$	$N = 7$	$N = 8$	$N = 9$	$N = 10$	$N = 11$	$N = 12$
$M = 1$	2.39	0.209	-2.26	0.432	1.41	0.730	0.894	0.834	0.851	0.846	0.847	0.847
$M = 2$	0.794	0.633	0.905	0.834	0.856	0.851	0.852	0.852	0.852	0.852	0.852	0.852
$M = 5$	0.868	0.827	0.852	0.850	0.850	0.850	0.850	0.850	0.850	0.850	0.850	0.850
$M = 10$	0.864	0.849	0.854	0.854	0.854	0.854	0.854	0.854	0.854	0.854	0.854	0.854
$M = 20$	0.859	0.852	0.854	0.854	0.854	0.854	0.854	0.854	0.854	0.854	0.854	0.854
$M = 40$	0.856	0.853	0.854	0.854	0.854	0.854	0.854	0.854	0.854	0.854	0.854	0.854
$M = 60$	0.855	0.853	0.854	0.854	0.854	0.854	0.854	0.854	0.854	0.854	0.854	0.854
$M = 80$	0.855	0.854	0.854	0.854	0.854	0.854	0.854	0.854	0.854	0.854	0.854	0.854
$M = 100$	0.855	0.854	0.854	0.854	0.854	0.854	0.854	0.854	0.854	0.854	0.854	0.854

$\bar{\sigma}_{\alpha\alpha}(a/2, b/2, h/2); R_\alpha/h = 10$												
	$N = 1$	$N = 2$	$N = 3$	$N = 4$	$N = 5$	$N = 6$	$N = 7$	$N = 8$	$N = 9$	$N = 10$	$N = 11$	$N = 12$
$M = 1$	-25.44	0.381	3.883	1.928	2.241	2.185	2.195	2.194	2.194	2.194	2.194	2.194
$M = 2$	4.943	1.541	2.317	2.219	2.232	2.232	2.232	2.232	2.232	2.232	2.232	2.232
$M = 5$	2.947	2.122	2.246	2.243	2.243	2.243	2.243	2.243	2.243	2.243	2.243	2.243
$M = 10$	2.563	2.214	2.245	2.245	2.245	2.245	2.245	2.245	2.245	2.245	2.245	2.245
$M = 20$	2.397	2.238	2.245	2.245	2.245	2.245	2.245	2.245	2.245	2.245	2.245	2.245
$M = 40$	2.319	2.243	2.245	2.245	2.245	2.245	2.245	2.245	2.245	2.245	2.245	2.245
$M = 60$	2.294	2.244	2.245	2.245	2.245	2.245	2.245	2.245	2.245	2.245	2.245	2.245
$M = 80$	2.282	2.245	2.245	2.245	2.245	2.245	2.245	2.245	2.245	2.245	2.245	2.245
$M = 100$	2.274	2.245	2.245	2.245	2.245	2.245	2.245	2.245	2.245	2.245	2.245	2.245

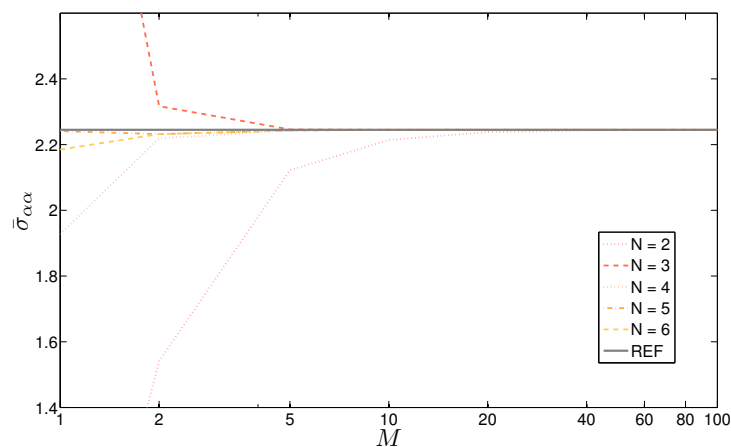


Figure 5. Case 2, simply supported composite laminated cylindrical shell with thickness ratio $R_\alpha/h = 10$. Stress $\bar{\sigma}_{\alpha\alpha}$ vs. number M of mathematical layers introduced for different orders of expansion N for the exponential matrix. REF means 3D solution by Ren [34].

The results presented in Table 5 are quite interesting. The considered case is the three-layered cylinder, with two different thickness ratios, which are $R_\alpha/h = 4$ and $R_\alpha/h = 10$. The dimensionless displacement \bar{w} and stress $\bar{\sigma}_{zz}$ are considered in the middle. These results show a faster convergence than that seen for the cylindrical panel. The moderately thick shell does not need the mathematical layers to be introduced, being convergent with just an expansion order of $N = 6$. At the same time, the solution for the thick cylinder converges with just $M = 5$ mathematical layers coupled with an

expansion order equal to $N = 4$. On the contrary, the cylindrical panel needed $M = 10$ mathematical layers coupled with $N = 3$ for the displacement and the stress to be convergent. For these effects, an important role is played by the symmetry of the cylinder geometry and its related bigger rigidity due to the closed geometrical form. The effect of the thickness in the convergence speed is clear in this case despite the fact that heterogeneous quantities are investigated. Some of the results of Table 5 are also shown in Figure 6 for the thinner shell. The curves were drawn for different and increasing values of order of expansion N .

Table 5. Case 3. Composite laminated cylinder. Displacement \bar{w} for thickness ratio $R_\alpha/h = 4$ and stress $\bar{\sigma}_{zz}$ for thickness ratio $R_\alpha/h = 10$, both evaluated in the middle and given as dimensionless values. Each physical layer ($N_L = 3$) is divided into M mathematical layers. 3D reference solution by Varadan and Bhaskar [15].

$\bar{w}(a/2, b/2, 0); R_\alpha/h = 4$												
	$N = 1$	$N = 2$	$N = 3$	$N = 4$	$N = 5$	$N = 6$	$N = 7$	$N = 8$	$N = 9$	$N = 10$	$N = 11$	$N = 12$
$M = 1$	4.436	1.668	6.346	2.967	4.578	3.820	4.085	3.999	4.023	4.017	4.019	4.018
$M = 2$	3.701	3.593	4.093	3.982	4.017	4.011	4.012	4.012	4.012	4.012	4.012	4.012
$M = 5$	3.952	3.974	4.012	4.009	4.009	4.009	4.009	4.009	4.009	4.009	4.009	4.009
$M = 10$	3.983	4.001	4.009	4.009	4.009	4.009	4.009	4.009	4.009	4.009	4.009	4.009
$M = 20$	3.997	4.007	4.009	4.009	4.009	4.009	4.009	4.009	4.009	4.009	4.009	4.009
$M = 40$	4.003	4.009	4.009	4.009	4.009	4.009	4.009	4.009	4.009	4.009	4.009	4.009
$M = 60$	4.005	4.009	4.009	4.009	4.009	4.009	4.009	4.009	4.009	4.009	4.009	4.009
$M = 80$	4.006	4.009	4.009	4.009	4.009	4.009	4.009	4.009	4.009	4.009	4.009	4.009
$M = 100$	4.007	4.009	4.009	4.009	4.009	4.009	4.009	4.009	4.009	4.009	4.009	4.009
$\bar{\sigma}_{zz}(a/2, b/2, 0); R_\alpha/h = 10$												
	$N = 1$	$N = 2$	$N = 3$	$N = 4$	$N = 5$	$N = 6$	$N = 7$	$N = 8$	$N = 9$	$N = 10$	$N = 11$	$N = 12$
$M = 1$	-1.72	-0.97	-1.35	-1.25	-1.28	-1.27	-1.27	-1.27	-1.27	-1.27	-1.27	-1.27
$M = 2$	-1.41	-1.20	-1.28	-1.27	-1.27	-1.27	-1.27	-1.27	-1.27	-1.27	-1.27	-1.27
$M = 5$	-1.32	-1.26	-1.27	-1.27	-1.27	-1.27	-1.27	-1.27	-1.27	-1.27	-1.27	-1.27
$M = 10$	-1.29	-1.27	-1.27	-1.27	-1.27	-1.27	-1.27	-1.27	-1.27	-1.27	-1.27	-1.27
$M = 20$	-1.28	-1.27	-1.27	-1.27	-1.27	-1.27	-1.27	-1.27	-1.27	-1.27	-1.27	-1.27
$M = 40$	-1.28	-1.27	-1.27	-1.27	-1.27	-1.27	-1.27	-1.27	-1.27	-1.27	-1.27	-1.27
$M = 60$	-1.27	-1.27	-1.27	-1.27	-1.27	-1.27	-1.27	-1.27	-1.27	-1.27	-1.27	-1.27
$M = 80$	-1.27	-1.27	-1.27	-1.27	-1.27	-1.27	-1.27	-1.27	-1.27	-1.27	-1.27	-1.27
$M = 100$	-1.27	-1.27	-1.27	-1.27	-1.27	-1.27	-1.27	-1.27	-1.27	-1.27	-1.27	-1.27

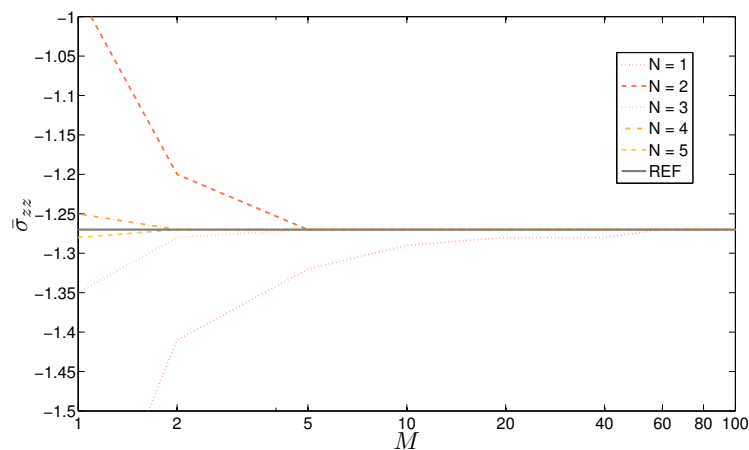


Figure 6. Case 3, simply supported composite laminated cylinder with thickness ratio $R_\alpha/h = 10$. Stress $\bar{\sigma}_{zz}$ vs. number M of mathematical layers introduced for different orders of expansion N for the exponential matrix. REF means 3D solution by Varadan and Bhaskar [15].

Table 6 is for the last case about a three-layered spherical shell. Only the displacement \bar{w} is investigated. The dimensionless values are given for a thick ($h/R_\alpha = 0.1$) and for a thin ($h/R_\alpha = 0.03$) structure. An increase in the expansion order of the exponential matrix is not sufficient without the

introduction of a certain number of mathematical layers. As the investigated quantity is the same in both cases (the displacement), this study easily investigates the effect of the thickness. The coupled values of M and N needed to obtain a better description of the phenomenon increase with the thickness. When the thickness is small (compared to the shell dimensions), $M = 2$ mathematical layers coupled with $N = 3$ allows for the solution to be reached. On the other side, the thicker shell needs at least $M = 5$ mathematical layers with an expansion of the exponential matrix equals $N = 5$. Figure 7 confirms the trend shown in Table 6 for the displacement \bar{w} of the thinner shell: the results move close to the exact value as the order of expansion is increased.

Table 6. Case 4. Composite laminated spherical shell. Displacement \bar{w} for thickness ratio $h/R_\alpha = 0.03$ and for thickness ratio $h/R_\alpha = 0.1$, both evaluated in the middle and given as dimensionless values. Each physical layer ($N_L=3$) is divided into M mathematical layers. 3D reference solution by Fan and Zhang [35].

$\bar{w}(a/2, b/2, 0); h/R_\alpha = 0.1$												
	$N = 1$	$N = 2$	$N = 3$	$N = 4$	$N = 5$	$N = 6$	$N = 7$	$N = 8$	$N = 9$	$N = 10$	$N = 11$	$N = 12$
$M = 1$	3.8504	3.3701	3.8261	3.7507	3.7658	3.7642	3.7644	3.7644	3.7644	3.7644	3.7644	3.7644
$M = 2$	3.7907	3.6788	3.7708	3.7652	3.7660	3.7659	3.7659	3.7659	3.7659	3.7659	3.7659	3.7659
$M = 5$	3.7732	3.7534	3.7666	3.7663	3.7664	3.7664	3.7664	3.7664	3.7664	3.7664	3.7664	3.7664
$M = 10$	3.7693	3.7633	3.7664	3.7664	3.7664	3.7664	3.7664	3.7664	3.7664	3.7664	3.7664	3.7664
$M = 20$	3.7678	3.7657	3.7664	3.7664	3.7664	3.7664	3.7664	3.7664	3.7664	3.7664	3.7664	3.7664
$M = 40$	3.7671	3.7662	3.7664	3.7664	3.7664	3.7664	3.7664	3.7664	3.7664	3.7664	3.7664	3.7664
$M = 60$	3.7669	3.7664	3.7664	3.7664	3.7664	3.7664	3.7664	3.7664	3.7664	3.7664	3.7664	3.7664
$M = 80$	3.7668	3.7664	3.7664	3.7664	3.7664	3.7664	3.7664	3.7664	3.7664	3.7664	3.7664	3.7664
$M = 100$	3.7667	3.7664	3.7664	3.7664	3.7664	3.7664	3.7664	3.7664	3.7664	3.7664	3.7664	3.7664

$\bar{w}(a/2, b/2, 0); h/R_\alpha = 0.03$												
	$N = 1$	$N = 2$	$N = 3$	$N = 4$	$N = 5$	$N = 6$	$N = 7$	$N = 8$	$N = 9$	$N = 10$	$N = 11$	$N = 12$
$M = 1$	0.4726	0.4540	0.4625	0.4623	0.4623	0.4623	0.4623	0.4623	0.4623	0.4623	0.4623	0.4623
$M = 2$	0.4665	0.4603	0.4624	0.4624	0.4624	0.4624	0.4624	0.4624	0.4624	0.4624	0.4624	0.4624
$M = 5$	0.4638	0.4620	0.4624	0.4624	0.4624	0.4624	0.4624	0.4624	0.4624	0.4624	0.4624	0.4624
$M = 10$	0.4631	0.4623	0.4624	0.4624	0.4624	0.4624	0.4624	0.4624	0.4624	0.4624	0.4624	0.4624
$M = 20$	0.4627	0.4624	0.4624	0.4624	0.4624	0.4624	0.4624	0.4624	0.4624	0.4624	0.4624	0.4624
$M = 40$	0.4625	0.4624	0.4624	0.4624	0.4624	0.4624	0.4624	0.4624	0.4624	0.4624	0.4624	0.4624
$M = 60$	0.4625	0.4624	0.4624	0.4624	0.4624	0.4624	0.4624	0.4624	0.4624	0.4624	0.4624	0.4624
$M = 80$	0.4625	0.4624	0.4624	0.4624	0.4624	0.4624	0.4624	0.4624	0.4624	0.4624	0.4624	0.4624
$M = 100$	0.4624	0.4624	0.4624	0.4624	0.4624	0.4624	0.4624	0.4624	0.4624	0.4624	0.4624	0.4624

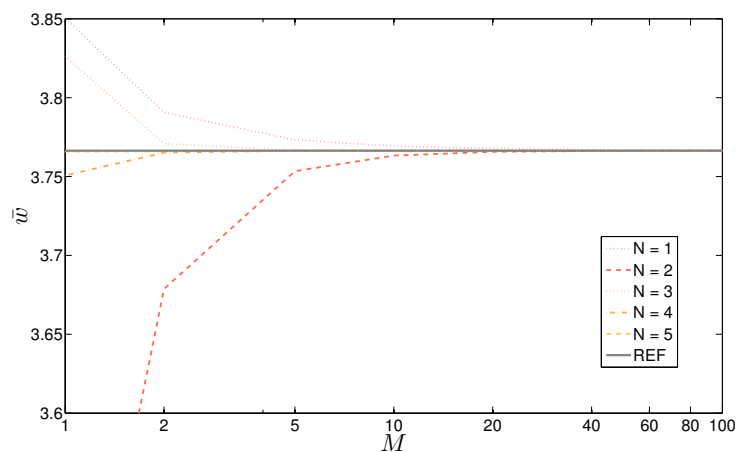


Figure 7. Case 4, simply supported composite laminated spherical shell with thickness ratio $h/R_\alpha = 0.1$. Displacement \bar{w} vs. number M of mathematical layers introduced for different orders of expansion N for the exponential matrix. REF means 3D solution by Fan and Zhang [35].

5. Conclusions

In this paper, a 3D solution for the static analysis of simply supported multilayered plates, cylinders and spherical/cylindrical shell panels is proposed. The three-dimensional equilibrium equations, written in mixed orthogonal curvilinear coordinates, are solved using the exponential matrix method and the assumption of a harmonic form for the displacement components. For a flat geometry, the coefficients of the differential equations are constant, allowing for reaching the solution by using just an opportune order of expansion N for the exponential matrix. When the curvature for shell geometries is introduced, an increase in the order of expansion N is not sufficient because the coefficients of the differential equations depend on the thickness coordinate z . For this reason, an opportune value M of mathematical layers must be introduced in each physical layer. This feature allows for solving differential equations with constant coefficients for each mathematical layer. An opportune combination of M and N values is necessary. Various parameters play a role in the definition of this optimum: the geometry, the thickness ratio, the material, the lamination sequence and the imposed half-wave numbers. For plates, there is no need for mathematical layers; the use of an order of expansion N for the exponential matrix equal to 12 allows for finding the correct solution even in the thicker cases. For shells, the partition of the physical layers into mathematical ones is the only way to calculate the curvature, and this feature is also useful for reducing the order of expansion N . As the co-role played by the various parameters in the convergence of the solution follows an unpredictable path, a conservative (but cost-effective) coupling of $N = 3$ and $M = 30$ may be used. With these proposed values, all of the investigated cases reach convergence for each arbitrary configuration. A significative influence of the thickness in the convergence speed is shown. As it increases, a higher value of N and/or M is needed. Convergence does not follow the same path for displacements and for stresses because the first ones are directly calculated from the equilibrium equations.

Author Contributions: Salvatore Brischetto implemented the analytical code; Roberto Torre analyzed the data; Salvatore Brischetto and Roberto Torre wrote the paper.

Conflicts of Interest: The authors declare no conflict of interest.

References

1. Tornabene, F.; Fantuzzi, N. *Mechanics of Laminated Composite Doubly-Curved Shell Structures. The Generalized Differential Quadrature Method and the Strong Formulation Finite Element Method*; Società Editrice Esculapio: Bologna, Italy, 2014.
2. Tornabene, F. *Meccanica delle Strutture a Guscio in Materiale Composito*; Società Editrice Esculapio, Bologna, Italy, 2012.
3. Gustafson, G.B. Systems of Differential Equations. Available online: <http://www.math.utah.edu/gustafso/2250systems-de.pdf> (accessed on 7 March 2016).
4. Molery C.; Van Loan, C. Nineteen dubious ways to compute the exponential of a matrix, twenty-five years later. *SIAM Rev.* **2003**, *45*, 1–46.
5. Pagano, N.J. Exact solutions for composite laminates in cylindrical bending. *J. Compos. Mater.* **1969**, *3*, 398–411.
6. Pagano, N.J. Exact solutions for rectangular bidirectional composites and sandwich plates. *J. Compos. Mater.* **1970**, *4*, 20–34.
7. Pagano N.J.; Wang, A.S.D. Further study of composite laminates under cylindrical bending. *J. Compos. Mater.* **1971**, *5*, 521–528.
8. Demasi, L. Three-dimensional closed form solutions and exact thin plate theories for isotropic plates. *Compos. Struct.* **2007**, *80*, 183–195.
9. Fan, J.; Ye, J. An exact solution for the statics and dynamics of laminated thick plates with orthotropic layers. *Int. J. Solids Struct.* **1990**, *26*, 655–662.
10. Srinivas, S.; Joga Rao, C.V.; Rao, A.K. An exact analysis for vibration of simply-supported homogeneous and laminated thick rectangular plates. *J. Sound Vib.* **1970**, *12*, 187–199.

11. Rokni Damavandi Taher, H.; Omid, M.; Zadpoor, A.A.; Nikooyan, A.A. Short Communication: Free vibration of circular and annular plates with variable thickness and different combinations of boundary conditions. *J. Sound Vib.* **2006**, *296*, 1084–1092.
12. Hosseini-Hashemi, S.; Salehipour, H.; Atashipour, S.R. Exact three-dimensional free vibration analysis of thick homogeneous plates coated by a functionally graded layer. *Acta Mech.* **2012**, *223*, 2153–2166.
13. Messina, A. Three dimensional free vibration analysis of cross-ply laminated plates through 2D and exact models. *Mech. Adv. Mater. Struct.* **2012**, *19*, 250–264.
14. Ye, J.Q. A three-dimensional free vibration analysis of cross-ply laminated rectangular plates with clamped edges. *Comput. Methods Appl. Mech. Eng.* **1997**, *140*, 383–392, .
15. Varadan, T.K.; Bhaskar, K. Bending of laminated orthotropic cylindrical shells—An elasticity approach. *Compos. Struct.* **1991**, *17*, 141–156.
16. Fan, J.-R.; Zhang, J.-Y. Exact solutions for thick laminated shells. *Sci. China* **1992**, *35*, 1343–1355.
17. Huang, N.N. Exact analysis for three-dimensional free vibrations of cross-ply cylindrical and doubly-curved laminates. *Acta Mech.* **1995**, *108*, 23–34.
18. Soldatos, K.P.; Ye, J. Axisymmetric static and dynamic analysis of laminated hollow cylinders composed of monoclinic elastic layers. *J. Sound Vib.* **1995**, *184*, 245–259.
19. Khalili, S.M.R.; Davar, A.; Malekzadeh, F.K. Free vibration analysis of homogeneous isotropic circular cylindrical shells based on a new three-dimensional refined higher-order theory. *Int. J. Mech. Sci.* **2012**, *56*, 1–25.
20. Brischetto, S. Three-dimensional exact free vibration analysis of spherical, cylindrical, and flat one-layered panels. *Shock Vib.* **2014**, *2014*, 479738.
21. Brischetto, S. An exact 3D solution for free vibrations of multilayered cross-ply composite and sandwich plates and shells. *Int. J. Appl. Mech.* **2014**, *6*, 1–42.
22. Brischetto, S. Exact three-dimensional static analysis of single- and multi-layered plates and shells. *Compos. Part B Eng.* **2017**, *119*, 230–252.
23. Brischetto, S. A closed-form 3D shell solution for multilayered structures subjected to different load combinations. *Aerosp. Sci. Technol.* **2017**, *70*, 29–46.
24. Brischetto, S. Convergence analysis of the exponential matrix method for the solution of 3D equilibrium equations for free vibration analysis of plates and shells. *Compos. Part B Eng.* **2016**, *98*, 453–471.
25. Brischetto, S. Exponential matrix method for the solution of exact 3D equilibrium equations for free vibrations of functionally graded plates and shells. *J. Sandw. Struct. Mater.* **2017**, doi:10.1177/1099636216686127.
26. Brischetto, S. Exact elasticity solution for natural frequencies of functionally graded simply-supported structures. *CMES Comput. Model. Eng. Sci.* **2013**, *95*, 391–430,
27. Hildebrand, F.B.; Reissner, E.; Thomas, G.B. *Notes on the Foundations of the Theory of Small Displacements of Orthotropic Shells*; NACA Technical Note No. 1833; NACA: Washington, DC, USA, 1949.
28. Soedel, W. *Vibration of Shells and Plates*; Marcel Dekker, Inc.: New York, NY, USA, 2004.
29. Reddy, J.N. *Mechanics of Laminated Composite Plates and Shells: Theory and Analysis*, 2nd ed.; CRC Press: New York, NY, USA, 2004.
30. Carrera, E.; Brischetto, S.; Nali, P. *Plates and Shells for Smart Structures: Classical and Advanced Theories for Modeling and Analysis*; John Wiley & Sons, Ltd.: New Delhi, India, 2011.
31. Boyce, W.E.; DiPrima, R.C. *Elementary Differential Equations and Boundary Value Problems*; John Wiley & Sons, Ltd.: New York, NY, USA, 2001.
32. Zwillinger, D. *Handbook of Differential Equations*; Academic Press: New York, NY, USA, 1997.
33. Brischetto, S. A general exact elastic shell solution for bending analysis of functionally graded structures. *Compos. Struct.* **2017**, *175*, 70–85.
34. Ren, J.G. Exact solutions for laminated cylindrical shells in cylindrical bending, *Compos. Sci. Technol.* **1987**, *29*, 169–187.
35. Fan, J.; Zhang, J. Analytical solutions for thick, doubly curved, laminated shells. *J. Eng. Mech.* **1992**, *118*, 1338–1356.

